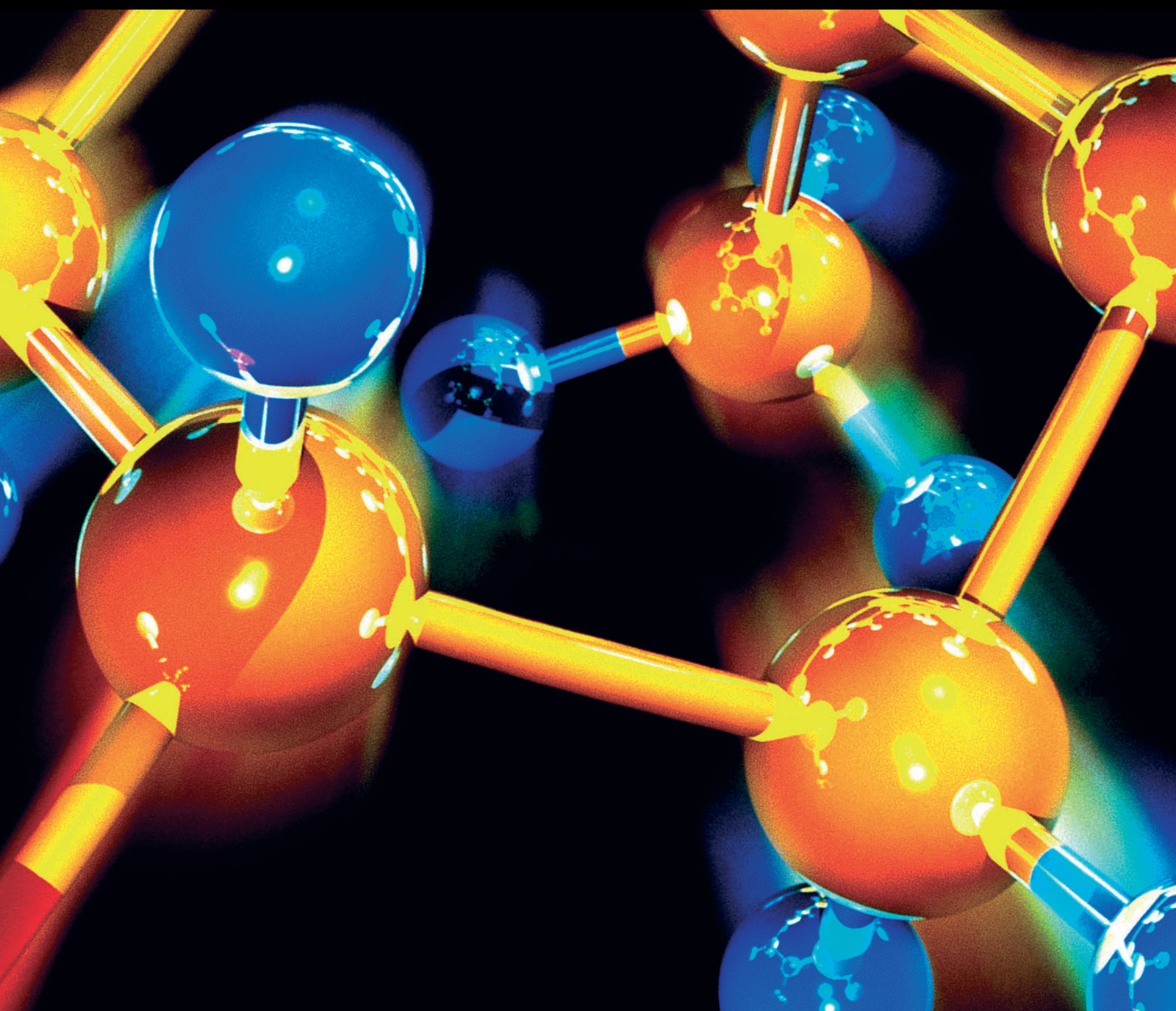# Highly Efficient Utilizations of Biomass for Energy and Catalysis

Lead Guest Editor: Gonggang Liu
Guest Editors: Shanshan Chang, Heng Jiang, Binghui Xu, and Zhifei Li

Highly Efficient Utilizations of Biomass for Energy and Catalysis

Highly Efficient Utilizations of Biomass for Energy and Catalysis

Lead Guest Editor: Gonggang Liu
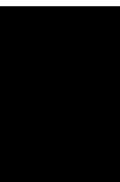Guest Editors: Shanshan Chang, Heng Jiang,
Binghui Xu, and Zhifei Li

Chief Editor

Kaustubha Mohanty, India

Associate Editors

Mohammad Al-Ghouti, Qatar
Tingyue Gu (iD), USA
Teodorico C. Ramalho (iD), Brazil
Artur M. S. Silva (iD), Portugal

Contents

Research Article

Uniform Loading of Nickel Phosphide Nanoparticles in Hierarchical Carbonized Wood Channel for Efficient Electrocatalytic Hydrogen Evolution

Yuanjuan Bai, Yidan Zhang, Shihong Cheng, Yongfeng Luo, Kun Du, Jinbo Hu, and Xianjun Li [ID]

Hunan Province Key Laboratory of Materials Surface & Interface Science and Technology,
College of Material Science and Engineering, Central South University of Forestry and Technology, Changsha 410004, China

Correspondence should be addressed to Xianjun Li; lxjmu@163.com

The development of self-supporting high-efficiency catalysts is a major challenge for the efficient production of H_2 via water splitting. In this manuscript, a freestanding Ni_2P-$Ni_{12}P_5$/carbonized wood (CW) composite electrode was prepared by a simple hydrothermal method and high-temperature calcination using pine wood with uniform channel as support and a large number of hydroxyl groups as nucleation center. The morphology and structural characteristics indicated that the Ni_2P and $Ni_{12}P_5$ nanoparticles were uniformly distributed within the hierarchical porous structure of the CW. In acid media, the as-prepared Ni_2P-$Ni_{12}P_5$/CW exhibits an excellent catalytic activity with a low overpotential of 151 mV at 10 mA cm^{-2} and a reasonably good long-term stability.

1. Introduction

In order to realize the sustainable development of human society in the future, how to develop and utilize economic new clean energy has become a main research direction in energy area in the 21st century [1–4]. Direct electrochemical water splitting under room temperature and pressure by using electrocatalyst seems to represent one of the most sustainable and clean strategies for H_2 production. [5, 6]. The best well-known electrocatalytic catalyst for hydrogen evolution reaction (HER) is the precious metal platinum, which has high cost and limited reserves. Therefore, many researchers are paying great attention to the development of high-efficiency, cheap, and environmental-friendly HER catalysts.

Nickel phosphide, which is characterized by high activity, low cost, and earth-abundant, is considered to be one of the most potential alternative HER catalysts for Pt [7–10]. Nevertheless, there is still plenty of scope for improvement in preparation ways and performance. For example, in the traditional process of synthesizing nickel phosphide [11–13], PH_3 gas released through phosphatization reaction is a highly toxic substance, which will seriously pollute the environment. Moreover, the poor conductivity of metal phosphide makes electron transport difficult, which is usually improved by the addition of conductive carbon [14, 15] or metallic element [16, 17].

Wood is a cheap, biodegradable biomass material with well-aligned channels in the growth direction. After proper physical and chemical treatment, they can be derived into wood-based micro/nanomaterials with controllable structure and adjustable performance. These features make them promising materials for numerous applications including energy conversion, wastewater treatments, and microwave absorption [18–20]. At present, wood trunk in electrocatalysis area is still in its infancy, but very promising. A large number of studies have shown that the original channel structure can be maintained after the wood is carbonized at high temperature [21–23]. The resulting carbonized wood-

(CW-) based composites with a certain amount of graphitized carbon have good electrical conductivity, which is conducive to rapid electron transmission along the channel directions. Besides, they can be used directly as a self-standing electrode [24] and provides a strong combination between active substances and CW, leading to enhanced electron transport and stability over the long-term operation. However, it is not easy to load nanoparticles evenly in wood channels.

In this work, we selected the pine wood with uniform and regular channels as raw material and synthesized a $Ni_2P-Ni_{12}P_5$/CW heterostructure composite through alkali treatment, hydrothermal reaction, and high-temperature calcination successively. Different from the traditional nongreen preparation method of transition metal phosphides with sodium phosphite or PH_3 gas as the phosphorus source, the nontoxic NaH_2PO_4 was employed as the phosphorus source and the Ni-P-O precursor was loaded into the wood channel by a simple hydrothermal method. Then, the resulting Ni-P-O wood composites were calcined in an inert gas at a high temperature to obtain a self-standing, additive-free $Ni_2P-Ni_{12}P_5$/CW electrode. The reason for the uniform loading of the active nanoparticles in the wood channels is that the abundant hydroxyl groups in the wood tracheid wall can act as the nucleation center of precursors. Impressively, the as-developed self-standing $Ni_2P-Ni_{12}P_5$/CW electrode shows an excellent catalytic performance toward HER.

2. Materials and Methods

2.1. Materials.
The pine wood was purchased from Chenzhou city, Hunan province, China. The reagents, including $NaH_2PO_4.2H_2O$, $Ni(NO_3)_2.6H_2O$, NH_4OH (≥28%), Na_2CO_3, H_2SO_4, NaOH, and Na_2SO_3, were purchased from Sinopharm Chemical Reagent Co, Ltd. Organic solvents, including ethylene glycol (AR) and absolute ethyl alcohol (AR), were obtained from Sigma Chemistry Co. Ltd. The deionized water was used to make up all mixed solutions and throughout the experiments.

2.2. Pretreatment of Pine Wood Slices.
The pine wood slices were cut into chips with a size of 2*2*0.2 cm along the radial direction by a copping saw. The obtained wood slices were immersed in a mixed solution of NaOH (1 M) and Na_2SO_3 (1 M) with the volume ratio of 1 : 1 at 80°C for 24 h and then washed the slices with ethanol and deionized (DI) water in an ultrasonic cleaner for 20 min to remove soluble inorganic salts and other trace elements. Finally, the pine wood slices were dried at 80°C for 24 h in vacuum.

2.3. Preparation of $Ni_2P-Ni_{12}P_5$/CW Composite Electrode.
The preparation process of the $Ni_2P-Ni_{12}P_5$/CW composite materials is shown schematically in Figure 1. Firstly, the Ni-P-O/wood composites were synthesized by a facile one-pot hydrothermal method. Typically, ethylene glycol (10 mL), NH_4OH (10 mL), an aqueous solution of Ni

$(NO_3)_2$ (5 mL, 1 M), an aqueous solution of NaH_2PO_4 (7.5 mL, 1 M), and an aqueous solution of Na_2CO_3 (5 mL, 1 M) were mixed step by step under vigorous stirring. During this process, it takes two minutes to add the next solution. The reaction solution was rapidly stirred in ambient air for 5 min after the last substance is added. Secondly, the above solution was transferred into a 50 mL Teflon-lined autoclave, and a piece of wood substrate was immersed into the reaction solution, which was maintained at 150°C for 24 h in an electric oven to produce Ni-P-O/wood composite precursors. From the XRD pattern in Figure 2(a), we can see the Ni-P-O/wood composite was constituted of ammonium nickel phosphate and nickel phosphate. In this process, because of the abundance of hydroxyl group in the wood channels, it can be served as nucleation for Ni-P-O growth and finally make the Ni-P-O uniform and stable load on the wood channels. This nucleation mechanism was also mentioned in our previous work [25, 26]. After the equipment cooled down to room temperature naturally, the wood slice was fetched out and ultrasonically cleaned using distilled water and ethanol several times in order to remove the product on the surface. After that, the wood slice loaded with Ni-P-O was dried in vacuum at 80°C overnight. Finally, the Ni-P-O/wood was converted to $Ni_2P-Ni_{12}P_5$/CW after calcining in Ar atmosphere at 800°C for 200 min. The digital photograph of Ni-P-O/wood and $Ni_2P-Ni_{12}P_5$/CW composites in Figure 2(b) shows the volume of wood block materials has shrunk and the particle has successfully loaded onto the surface of the wood after calcination at high temperature.

2.4. Characterization.
The morphologies and elemental analysis of the $Ni_2P-Ni_{12}P_5$/CW material were characterized using a scanning electron microscope (SEM, JSM-7800F, JEOL) equipped with an energy dispersive spectrometer (EDS). The crystal structures and phase characterization of them were measured by an X-ray diffractometer (X'Pert PRO, PANalytical) in the range of 5–90° (2θ). The specific surface area and pore distribution were examined using nitrogen adsorption and desorption isotherms on an automatic surface area and porosity analyzer (ASAP 2460, Micromeritics). The degree of graphitization of CW was conducted on a LabRAM HR Evolution (HORIBA Jobin Yvon SAS).

2.5. HER Experiments.
All electrochemical tests were performed on CHI 760E chemical workstation (CH Instruments, Inc., Shanghai) using a typical three-electrode setup, with the graphite rod, saturated calomel electrode, and self-standing $Ni_2P-Ni_{12}P_5$/CW acting as the counter, reference, and working electrode, respectively. Linear sweep voltammetry (LSV) was performed on a solution of $0.5 M \cdot H_2SO_4$ with a scan rate of $5 mV \cdot s^{-1}$. All potentials measured were calibrated to RHE using the following equation: E (RHE) = E (SCE) + 0.059 × pH + 0.242. All experiments were carried out at room temperature (~25°C).
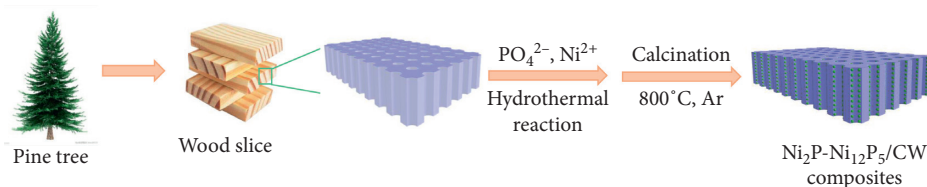
FIGURE 1: Schematic illustration of preparing the Ni_2P-$Ni_{12}P_5$/CW composite materials.

(a)

(b)

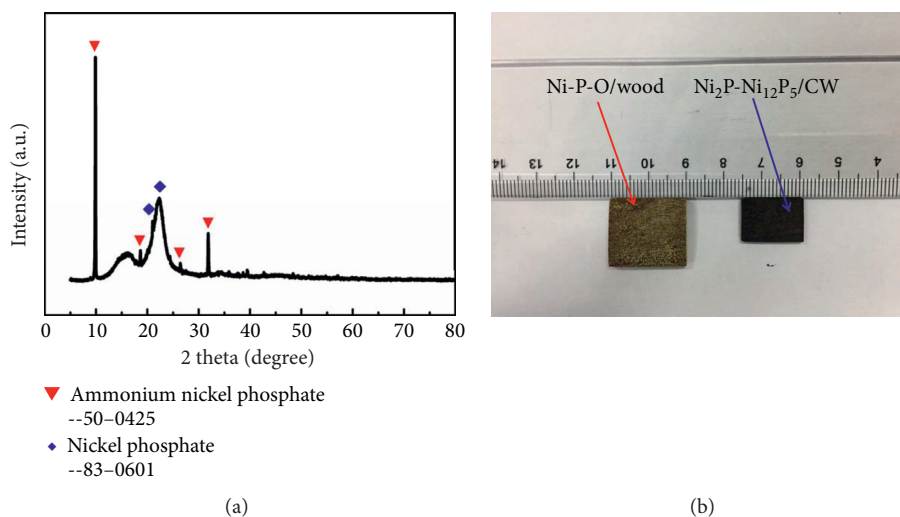FIGURE 2: (a) Powder XRD pattern of the Ni-P-O precursors. (b) Digital photograph of Ni-P-O/wood and Ni_2P-$Ni_{12}P_5$/CW composites.

3. Results and Discussion

3.1. Phase, Morphology, Chemical Composition, and Structure Study of Ni_2P-$Ni_{12}P_5$/CW

3.1.1. XRD. At first, the crystal structure of the as-prepared products was characterized by the XRD patterns as shown in Figure 3. The samples show a set of obvious peaks at 40.7°, 44.6°, 47.4°, 54.2°, 55.0°, and 74.8°, corresponding to (111), (201), (210), (300), (211), and (400) of Ni_2P (JCPDS: 74–1385), respectively, suggesting the end-products containing hexagonal Ni_2P. Previous research studies have shown that Ni_2P is one of the best catalysts for HER. In addition, the samples also include another phase, which can be indexed to the tetragonal $Ni_{12}P_5$ (JCPDS: 22–1190). The diffraction peaks of both Ni_2P and $Ni_{12}P_5$ were sharp and intense, indicating their highly crystalline nature. Besides, we can see a broad peak at 23.4° and a weak peak at 26.4° in the pattern, which can be ascribed to the amorphous and graphitized carbon features of the CW block. These results indicate the obtained product is a composite material composed of Ni_2P, $Ni_{12}P_5$, and CW.

3.1.2. SEM and EDS. Figure 4 shows some typical SEM images. From Figure 4(a), we can see clearly many straight channels along the growth direction of pine tree and the straight channels have different diameters and numerous small channels around the big channels. Figures 4(b) and 4(c) reveal that the Ni_2P-$Ni_{12}P_5$ nanoparticles are evenly
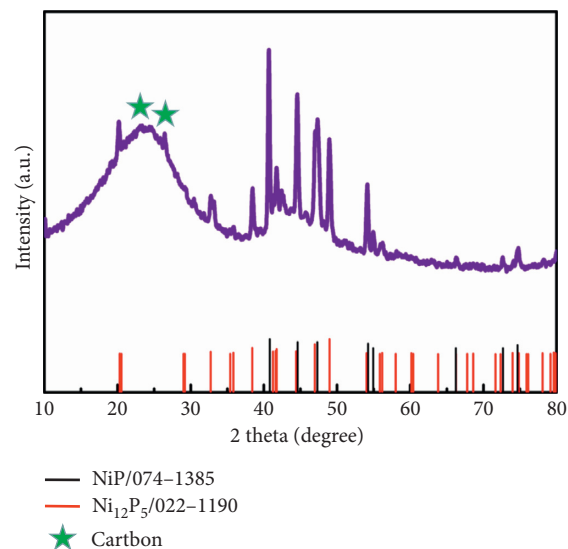
FIGURE 3: XRD patterns of Ni_2P-$Ni_{12}P_5$/CW composites.

dispersed in the CW's channels, and the size of nanoparticle is about 80 nm. Furthermore, the EDS data from Figure 5 demonstrate that the Ni_2P-$Ni_{12}P_5$/CW electrode mainly consists of Ni, P, and C elements. The trace amount of O element may be due to the material's exposure to the air. And the corresponding quantitative analysis of elements shows the atom ration of P/Ni = 1/3. After calculation, the molar ratio of Ni_2P to $Ni_{12}P_5$ is about 1/7.

(a)   (b)   (c)
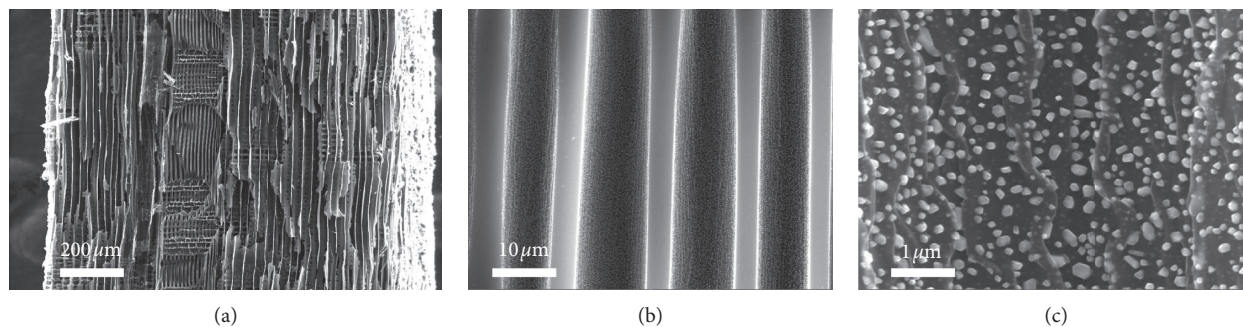
FIGURE 4: SEM images of $Ni_2P-Ni_{12}P_5/CW$ at different magnifications.

Element (%)	Weight (%)	Atom (%)
C	88.97	94.22
O	5.61	4.46
P	0.74	0.30
Ni	4.68	1.01
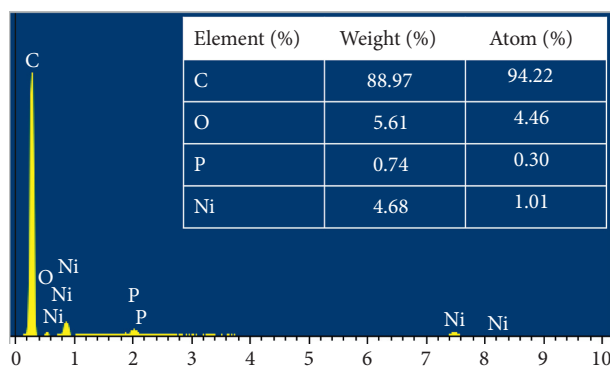
FIGURE 5: EDS spectra and element content analysis table of $Ni_2P-Ni_{12}P_5/CW$.

(a)   (b)   (c)
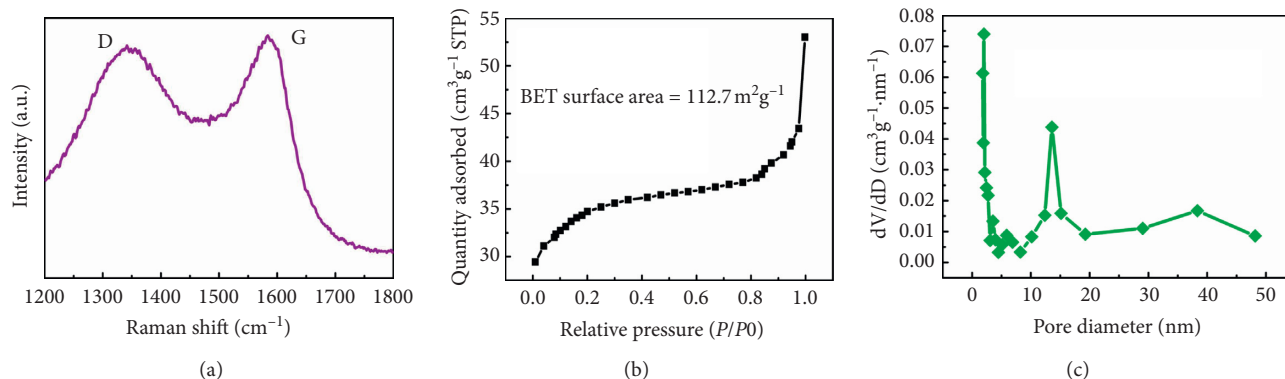
FIGURE 6: (a) Raman spectrum and (b, c) nitrogen adsorption-desorption isotherm of the prepared $Ni_2P-Ni_{12}P_5/CW$.

3.1.3. Raman Spectrum and Surface Area Study of Ni_2P-$Ni_{12}P_5/CW$.

The Raman spectroscopy of the CW slice loading $Ni_2P-Ni_{12}P_5$ nanoparticles is presented in Figure 6(a). In the spectra, there are two characteristic bands: D band at around $1340 \, cm^{-1}$ and G band at about $1590 \, cm^{-1}$, respectively, match well with amorphous and graphitized carbons. In theory, when the temperature of calcination reaches 800°C, some of the carbon in CW slice will be converted to graphitized carbon. As expected, the I_G/I_D ratio is about 1.05, which suggests good crystallization of the $Ni_2P-Ni_{12}P_5/CW$ obtained after 800°C annealing. Nitrogen absorption/desorption analysis was applied to investigate the Brunauer–Emmett–Teller (BET) surface area and pore

diameter of the $Ni_2P-Ni_{12}P_5/CW$ samples. From Figure 6(b), we can see the BET surface area of the $Ni_2P-Ni_{12}P_5/CW$ is about $112.7 \, m^2 \cdot g^{-1}$. And this material has hierarchical pore structure, as shown in Figure 6(c).

3.2. Electrochemical Performance Study of Ni_2P-$Ni_{12}P_5/CW$.

The HER catalytic activity of the integrated $Ni_2P-Ni_{12}P_5/CW$ electrode is evaluated in $0.5 \, M \cdot H_2SO_4$ solution using a three-electrode cell. And using the acid corrosion method, the load mass of the active substances of the $Ni_2P-Ni_{12}P_5/CW$ electrode could be calculated to be about $0.36 \, mg \cdot cm^{-2}$. Figure 7(a) displays the polarization curves of the Ni_2P-

(a)

(b)

(c)

FIGURE 7: (a) Polarization curves and (b) Tafel plots calculated from polarization curves of the Ni_2P-$Ni_{12}P_5$/CW electrode in 0.5 M·H_2SO_4 at room temperature with a scan rate of 5 mV·s^{-1}. (c) Chronoamperometric profile of the electrode measured at −200 mV in 0.5 M·H_2SO_4.

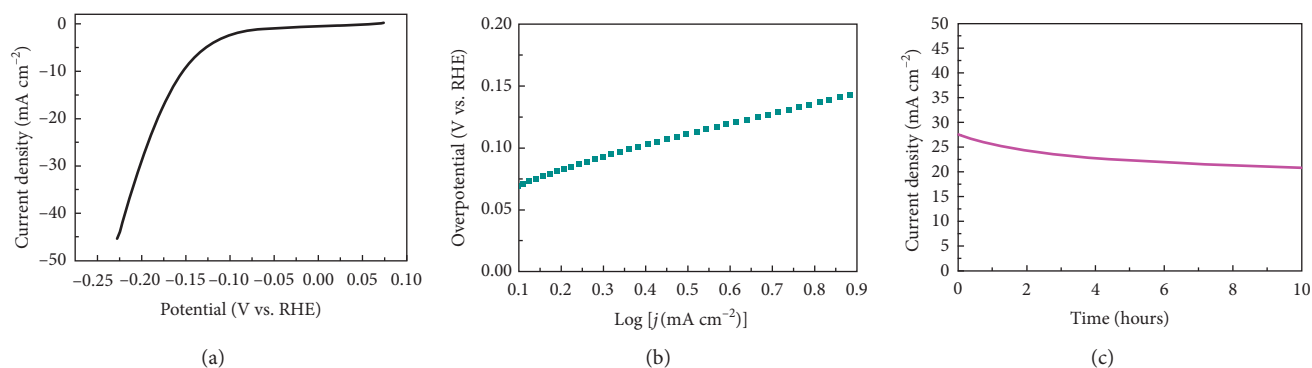$Ni_{12}P_5$/CW electrode. As expected, the Ni_2P-$Ni_{12}P_5$/CW electrode exhibits a good HER activity and achieved a current density of 10 mA·cm^{-2} at a low overpotential of 151 mV. Further insight into the catalytic activity of Ni_2P-$Ni_{12}P_5$/CW is obtained by extracting the slopes from the Tafel plots in Figure 7(b). The calculated value of Tafel slopes is about 79 mV dec^{-1}, which suggests that HER on Ni_2P-$Ni_{12}P_5$/CW occurs via a Volmer–Heyrovsky mechanism. In addition, the Ni_2P-$Ni_{12}P_5$/CW electrode also exhibits strong durability in strong acid media (Figure 7(c)). Based on the above discussion and experimental results, the reasons for the superior properties of Ni_2P-$Ni_{12}P_5$/CW can be ascribed to the following points. Firstly, abundant channels in the CW provide a large specific surface area, facilitating electrolyte infiltration. Secondly, the graphitized carbon of the Ni_2P-$Ni_{12}P_5$/CW has excellent electrical conductivity, which is conducive to rapid electron transport. Thirdly, this self-supporting electrode of Ni_2P-$Ni_{12}P_5$/CW allows electrons to move quickly between the electrode and the active material.

4. Conclusions

In this work, we chose a cheap biomass material pine wood as the raw material and introduced Ni-P-O precursors by a hydrothermal method using a large number of hydroxyl groups in the wood channel as the nucleation center. After a high-temperature calcination process, a self-supporting Ni_2P-$Ni_{12}P_5$/CW electrode with Ni_2P-$Ni_{12}P_5$ nanoparticles evenly dispersed in the CW channels was obtained. With the highly porous feature, large surface area, good electrical conductivity, extended electronic structure, and preeminent structural stabilization of CW, the Ni_2P-$Ni_{12}P_5$/CW electrode exhibits excellent HER activity and stability.

Data Availability

The data used to support the findings of this study are included within the article.

Conflicts of Interest

The authors declare that they have no conflicts of interest.

Acknowledgments

References

[1] U.S. Energy Information Administration, *International Energy Outlook*, U.S. Energy Information Administration, Washington, D.C., USA, 2016.

[2] British Petroleum, "Statistical review of world energy," British Petroleum, London, UK, 2017.

[3] B. Dunn, H. Kamath, and J.-M. Tarascon, "Electrical energy storage for the grid: a battery of choices," *Science*, vol. 334, no. 6058, pp. 928–935, 2011.

[4] W. Li, J. Liu, and D. Zhao, "Mesoporous materials for energy conversion and storage devices," *Nature Reviews Materials*, vol. 1, p. 16023, 2016.

[5] L. Rößner and M. Armbrüster, "Electrochemical energy conversion on intermetallic compounds: a review," *ACS Catalysis*, vol. 9, no. 3, pp. 2018–2062, 2019.

[6] D. A. Henckel, M. HenckelOlivia, O. M. Lenz, K. M. Krishnan, and B. M. Cossairt, "Improved HER catalysis through facile, aqueous electrochemical activation of nanoscale WSe2," *Nano Letters*, vol. 18, no. 4, pp. 2329–2335, 2018.

[7] C. Cossairt, R. Zhang, and W. Lu, "Energy-saving electrolytic hydrogen generation: Ni2P nanoarray as a high-performance non-noble-metal electrocatalyst," *Angewandte Chemie*, vol. 129, no. 3, pp. 860–864, 2017.

[8] J. Sun, Y. Chen, Z. Ren et al., "Self-supported NiS nanoparticle-coupled Ni_2P nanoflake array architecture: an advanced catalyst for electrochemical hydrogen evolution," *ChemElectroChem*, vol. 4, pp. 1–9, 2017.

[9] H. Wen, L.-Y. Gan, H.-B. Dai et al., "In situ grown Ni phosphide nanowire array on Ni foam as a high-performance catalyst for hydrazine electrooxidation," *Applied Catalysis B: Environmental*, vol. 241, pp. 292–298, 2019.

[10] R. Zhang, P. A. Russo, M Feist, P. Amsalem, N. Koch, and N. Pinna, "Synthesis of nickel phosphide electrocatalysts from hybrid metal phosphonates," *ACS Applied Materials & Interfaces*, vol. 9, no. 16, pp. 14013–14022, 2017.

[11] L.-A. Stern, L. Feng, F. Song, and X. Hu, "Ni2P as a Janus catalyst for water splitting: the oxygen evolution activity of Ni2P nanoparticles," *Energy & Environmental Science*, vol. 8, no. 8, pp. 2347–2351, 2015.

[12] A. Dutta, A. K. Samantara, S. K. Dutta, B. K. Jena, and N. Pradhan, "Surface-oxidized dicobalt phosphide nano-needles as a nonprecious, durable, and efficient OER catalyst," *ACS Energy Letters*, vol. 1, no. 1, pp. 169–174, 2016.

[13] J. Chang, L. Liang, C. Li et al., "Ultrathin cobalt phosphide nanosheets as efficient bifunctional catalysts for a water electrolysis cell and the origin for cell performance degradation," *Green Chemistry*, vol. 18, no. 8, pp. 2287–2295, 2016.

[14] Y. Li, P. Cai, S. Ci, and Z. Wen, "Strongly coupled 3D nanohybrids with Ni2 P/carbon nanosheets as pH-universal hydrogen evolution reaction electrocatalysts," *ChemElectroChem*, vol. 4, no. 2, pp. 340–344, 2017.

[15] J. Chang, Y. Xiao, M. Xiao, J. Ge, C. Liu, and W. Xing, "Surface oxidized cobalt-phosphide nanorods as an advanced oxygen evolution catalyst in alkaline solution," *ACS Catalysis*, vol. 5, no. 11, pp. 6874–6878, 2015.

[16] Y. Lian, H. Sun, X. Wang et al., "Carved nanoframes of cobalt-iron bimetal phosphide as a bifunctional electrocatalyst for efficient overall water splitting," *Chemical Science*, vol. 10, no. 2, pp. 464–474, 2019.

[17] Q. Sun, M. Zhou, Y. Shen et al., "Hierarchical nanoporous Ni (Cu) alloy anchored on amorphous NiFeP as efficient bifunctional electrocatalysts for hydrogen evolution and hydrazine oxidation," *Journal of Catalysis*, vol. 373, pp. 180–189, 2019.

[18] Y. Wang, G. Sun, J. Dai et al., "A high-performance, low-tortuosity wood-carbon monolith reactor," *Advanced Materials*, vol. 29, no. 2, p. 1604257, 2017.

[19] L. A. Berglund and I. Burgert, "Bioinspired wood nanotechnology for functional materials," *Advanced Materials*, vol. 30, no. 19, p. 1704285, 2018.

[20] J. Song, C. Chen, S. Zhu et al., "Processing bulk natural wood into a high-performance structural material," *Nature*, vol. 554, no. 7691, pp. 224–228, 2018.

[21] Y. Li, M. Cheng, E. Jungstedt, B. Xu, L. Sun, and L. Berglund, "Optically transparent wood substrate for perovskite solar cells," *ACS Sustainable Chemistry & Engineering*, vol. 7, no. 6, pp. 6061–6067, 2019.

[22] S. Zhang, C. Wu, W. Wu et al., "High performance flexible supercapacitors based on porous wood carbon slices derived from Chinese fir wood scraps," *Journal of Power Sources*, vol. 424, pp. 1–7, 2019.

[23] Q. W. Jiang, G. R. Li, F. Wang, and X. P. Gao, "Highly ordered mesoporous carbon arrays from natural wood materials as counter electrode for dye-sensitized solar cells," *Electrochemistry Communications*, vol. 12, no. 7, pp. 924–927, 2010.

[24] H. S. Yaddanapudi, K. Tian, S. Teng, and A. Tiwari, "Facile preparation of nickel/carbonized wood nanocomposite for environmentally friendly supercapacitor electrodes," *Scientific Reports*, vol. 6, p. 33659, 2016.

[25] Y. Bai, H. Zhang, L. Fang, L. Liu, H. Qiu, and Y. Wang, "Novel peapod array of Ni2P@graphitized carbon fiber composites growing on Ti substrate: a superior material for Li-ion batteries and the hydrogen evolution reaction," *Journal of Materials Chemistry A*, vol. 3, no. 10, pp. 5434–5441, 2015.

[26] Y. Bai, L. Fang, H. Xu, X. Gu, H. Zhang, and Y. Wang, "Strengthened synergistic effect of metallic MxPy (M=Co, Ni, and Cu) and carbon layer via peapod-like architecture for both hydrogen and oxygen evolution reactions," *Small*, vol. 13, no. 16, p. 1603718, 2017.

Research Article

Removal of Nutrients from Fertilizer Plant Wastewater Using *Scenedesmus* sp.: Formation of Bioflocculation and Enhancement of Removal Efficiency

Thanh-Luu Pham [ID] [1,2] **and Manh Ha Bui** [ID] [3,4]

[1]*Ho Chi Minh City University of Technology (HUTECH), 475A Dien Bien Phu Street, Ward 25, Binh Thanh District, Ho Chi Minh City 700000, Vietnam*
[2]*Institute of Tropical Biology, Vietnam Academy of Science and Technology (VAST), 85 Tran Quoc Toan Street, District 3, Ho Chi Minh City 700000, Vietnam*
[3]*Institute of Research and Development, Duy Tan University, 182 Nguyen Van Linh Street, Thanh Khe District, Da Nang City 550000, Vietnam*
[4]*Department of Environmental Science, Saigon University, 273 An Duong Vuong Street, District 5, Ho Chi Minh City 700000, Vietnam*

Correspondence should be addressed to Thanh-Luu Pham; pt.luu@hutech.edu.vn

Eutrophication of surface water has become an environmental concern in recent decades. High concentrations of nutrients, especially nitrogen- and phosphorus-rich species, have contributed to the process of eutrophication, highlighting a demand for effective and economical methods of removing nitrogen and phosphorus from wastewater. This study aimed to investigate the ability of a green microalga species, *Scenedesmus* sp., to remove nitrogen and phosphorus, as well as chemical oxygen demand (COD) and biochemical oxygen demand (BOD_5), from fertilizer plant wastewater. Different microalgae concentrations from 10 mg/L to 60 mg/L were used to assess the growth rate, biomass production, and removal ability. The results indicated that *Scenedesmus* sp. grew well in the wastewater (with a growth rate from 0.3 to 0.38/day) and produced up to 70.2 mg/L of dry biomass. The algal species was able to remove ammonium (NH_4^+), nitrate (NO_3^-), phosphate (PO_4^{3-}), total phosphorus (TP), COD, and BOD_5 with removal rates up to 93%, 84%, 97%, 96%, 93%, and 84%, respectively. Autobioflocculation (AFL) was observed in all cultures with flocculation activity of up to 88.3% in the highest algal biomass treatment. The formation of bioflocculation enhanced the removal of nutrients, COD, and BOD_5 from wastewater effluent. The results indicated that wastewater from a fertilizer plant could be used as a cost-effective growth medium for algal biomass. The autoflocculation of microalgae could be used as a more practical approach for wastewater treatment using microalgae to eliminate eutrophication.

1. Introduction

In recent decades, the intensity of agricultural and industrial activities, together with rapid urbanization, has generated large amounts of wastewaters [1]. The continuous disposal of wastewaters without appropriate treatment to water sources has posed severe water pollution problems, especially in developing countries [2]. These effluents contain a high concentration of nutrients such as nitrogen and phosphorus, which are the leading causes of eutrophication in natural waters [3]. This condition is favorable for the development of harmful algal blooms (HABs) resulted in the degradation of water quality and impairment of freshwater ecosystems [4]. Moreover, the occurrence of HABs can result in serious problems such as anoxic conditions, toxin productions, killing of fish, and altered biodiversity [5]. HABs are considered a public health risk due to produce a variety of toxic secondary metabolisms [6]. For these reasons, many efforts

have been done in order to mitigate eutrophication by reducing nitrogen and phosphorus concentration in wastewater effluents before discharging into water sources.

To mitigate eutrophication, nutrient control is a fundamental process [7]. Physical and chemical methods have been developed for the removal of nutrients from wastewater, but these are costly and produce high sludge content [8]. Due to requiring large amounts of the nutrient, especially nitrogen and phosphorus for growth, many species of green microalgae such as *Chlorella* sp., *Scenedesmus* sp., and *Neochloris* sp. have been proposed as an alternative biological treatment to remove nitrogen and phosphorus from a different sources of wastewater for many years [2, 8, 9]. Indeed, extensive studies have been carried out on the subject of microalgae cultivation using wastewater. High removal efficiencies of nitrogen and phosphorus (more than 80%) from wastewaters of different sources have already been recorded for several microalgae species [9–12].

Recent evidence indicated that the formation of microalgae-bacteria flocculation (MBF) and fungi-assisted microalgae pellets (FAMP) enhanced nutrient removal from wastewater effluent [13, 14]. While MBF is a flocculation formation of microalgae cells assisted with bacteria, FAMP is a pellet formation of microalgae cells supported with fungi [14, 15]. During bioflocculation formation, the aggregation of bacteria or fungi and microalgae cells creates large flocs or pellets which accelerate the adsorption of suspended compounds in surrounding medium to form co-bioflocculate and thus enhance the removal efficiency of nitrogen and phosphorus [14–16]. Therefore, MBF and FAMP have been used to improve nutrient removal and effluent recovery in aerobic-activated sludge technologies [13, 15, 17]. The bioflocculation of microalgae and bacteria have been intensively studied and reviewed for recent advances and perspectives [18–20]. Besides, MBF can be used as a promising low-cost method for harvesting microalga biomass [14, 21].

Another flocculation can occur naturally in certain microalgae in response to some environmental stress, which is so-called autoflocculation (AFL) [14]. However, little is known about AFL of microalgae. Moreover, the driving factor for the formation of AFL is not understood yet. Therefore, it is vital to pay more attention to the technique to obtain more knowledge about AFL formation and enhance its application.

The fertilizer industry is one of the most important economic sectors in Vietnam due to its economy is based on agriculture. Wastewaters from fertilizer plants contained a variety of nutrients include nitrogen and phosphorous compounds that is a significant problem of water eutrophication [22]. In the present study, wastewater effluent obtained from Phu My Fertilizer Plant (Vietnam) was used as a culture medium for microalgae production. The present study aimed to investigate the nutrient removal ability of a native microalga *Scenedesmus* sp. species. Furthermore, the biomass growth, flocculating activity, chemical oxygen demand (COD) and biochemical oxygen demand (BOD$_5$) removal, dry matter and chlorophyll content of the flocs collected, and the wastewater nutrient removal were studied in order to evaluate the potential use of the microalgae for controlling eutrophication and producing renewable energy.

2. Materials and Methods

2.1. Wastewater Sample Collection and Characterization.
The wastewater used in the present study was collected from equation tanks (ET) in the Phu My Fertilizer Wastewater Plant (Vietnam). Samples for wastewater characterization were immediately stored at 4°C prior to analysis. The microalgae sample was collected from a similar ET by using a phytoplankton net. Dissolved oxygen (DO), temperature, and water pH were measured *in situ* with a multiparameter meter (Hach 156, USA). Before using for all the experiments throughout this study, the wastewater was filtered through 0.45 μm filters to remove the suspended grease layer.

2.2. Isolation of Microalgae from Wastewater.
The microalgae sample was enriched separately in different flasks with COMBO medium [23] prior to isolation. Samples were screened under a microscope. *Scenedesmus* sp. was dominant in wastewater. Colonies of *Scenedesmus* sp. (Figure 1) were isolated by micropipetting and washing. All cultures were maintained under laboratory conditions at a temperature of 27°C, 12 h light photoperiods, and light intensity of 50 μmol photons/m^2/s. The axenic strains were cultured in conical flasks containing a sterile liquid medium.

The microalgae biomass was measured using the gravimetric method. A 20 mL sample was placed in a preweighed glass tube. After centrifugation at 4000 rpm for 15 minutes, the supernatant was discarded, and then the tubes were dried at 105°C for 24 hours and reweighted. The dry biomass was calculated gravimetrically by weight difference. Samples were prepared in triplicate for calculation of the standard errors.

2.3. Experimental Setup.
Precultures showed that *Scenedesmus* sp. grew well in cultured medium at room temperature (27 ± 1°C) under 12 hour photoperiods with the light intensity of 95 μmol photons/m^2/s. Therefore, this condition was selected for conducting the experiments. Batch experiments were conducted in triplicate with an initial pH of 7.3 ± 0.5 (no pH control) by using 1000 mL flasks placed in a shaker at 70 rpm. Each flask with 800 mL of wastewater inoculated with a suspension of precultured cells. The initial biomass was prepared at 10, 20, 30, 40, and 60 mg dry weight (DW)/L. Illumination was provided continuously by linear fluorescent lamps using 12 hour photoperiods for 10 days. The flasks containing wastewater without microalgae cells were used as controls. The single-isolated microalga was used for the experiment. 1 mL sample was collected every day to determine optical density. Samples for measurement nutrients concentration were prepared by withdrawing 100 mL from flasks at three-day interval. And then, the samples were centrifuged at 5000 rpm for 10 min to remove the microalga cells, and the supernatant was collected for analysis of nutrients concentration in the same

FIGURE 1: Morphology of colonies of *Scenedesmus* sp. under a microscope. Scale bar: 20μm.

days. Dry microalga biomass and total lipid content were determined at the beginning and end of the bioassays.

2.4. Measurement of the Growth Rate and Flocculation Activity.

The growth rate (GR) of the microalgae was calculated as follows:

$$GR = \ln \frac{(N_t/N_0)}{(T_t - T_0)}, \tag{1}$$

where N_t and N_0 are the microalgae biomass (mg/L) at the end (T_t) and start (T_0) of the growth phase, respectively.

The flocculation activity (FA) was measured according to the method reported previously by Nguyen et al. [13] as follows:

$$FA (\%) = \left(1 - \frac{OD_{680t}}{OD_{680t0}}\right) \times 100, \tag{2}$$

where OD_{680t} is the optical density of the sample at time t and OD_{680t0} is the optical density at time t_0.

2.5. Chlorophyll Content.

To determine the chlorophyll (Chl) content of microalgae, a known volume of culture samples (1 mL) was centrifuged at 5000 rpm for 10 min. After discarding the supernatant, Chl from microalgae cells was extracted with 3 mL of methanol (100%) overnight in the dark at room temperature. Then, the suspension was centrifuged at 10000 rpm for 10 min to remove the cell debris. After centrifugation, the supernatant was used to measure Chl content 652 nm (Chl-b), 665 nm (Chl-a), and 750 nm (turbidity of suspension) by using a spectrophotometer (UV-VIS, Harch, 500), and the concentration of Chl (μg/mL) was calculated as follows [24]:

$$Chl = \left[-8.0962 \left(OD_{652} - OD_{750}\right) + 16.5169 \left(OD_{665} - OD_{750}\right)\right] \frac{V_2}{V_1 l}, \tag{3}$$

where V_1 and V_2 are the volume of sample suspension and methanol used, respectively. And, l is the optical path, which is 1 cm.

2.6. Measurement of Wastewater Quality Parameters.

Wastewater quality parameters including ammonium (NH_4^+), nitrate (NO_3^-) and phosphate (PO_4^{3-}), total nitrogen (TN), total phosphate and total suspended solids (TSS), biochemical oxygen demand (BOD_5), and chemical oxygen demand (COD) were analyzed according to the Standard Methods for Examination of Water and Wastewater [25].

The efficiency of nutrient removal (E_r) in wastewater was expressed in

$$E_r (\%) = \frac{C_o - C_f}{C_o} \times 100, \tag{4}$$

where C_o and C_f are the initial and final concentrations of nutrients concentration in wastewater effluent.

2.7. Statistical Analysis.

The differences between mean values of the specific growth rate, dry microalga biomass, and pollutant removal rates were tested for significance using a one-way analysis of variance (ANOVA). P values ≤ 0.05 were considered significant differences. All results are presented in the form of mean values $\pm$ standard deviation from three samples.

3. Results and Discussion

3.1. Characteristics of Wastewater.

The wastewater used for the experiment was analyzed for evaluating physico-chemical characteristics. The physico-chemical parameters of the wastewater, including pH, temperature, main nutrient species, as well as BOD_5 and COD were presented in Table 1. The wastewater effluent collected from the Phu My Fertilizer Plant contained large amounts of nitrogen (47.3 ± 5.9 mg/L) in the form of ammonium (NH_4^+) and nitrate (NO_3^-) with small amounts of phosphate (PO_4^{3-}) (0.9 ± 0.28 mg/L). Besides, the initial pH of the wastewater effluent was almost constant at pH 6.8. Ammonium is among the most common chemical forms of nitrogen that can be readily absorbed by most microalga species [26]. The concentration of phosphorus was also found sufficient to support algal growth. In this respect, the effluent collected from the Phu My Fertilizer Wastewater Treatment Plant could be used as a cheap source of nutrients for microalgal cultivation. The characterized of the raw wastewater was noted to be favorable for microalgae growth. A ratio of COD/TN/TP, i.e., 180/47/2, found with this wastewater, is suitable for nutrient removal with microalgae. The BOD_5/TP, BOD_5/PO_4^{3--}, and PO_4^{3-}/TP ratios were found to be reasonably high (Table 1). The optimal inorganic N/P ratio for freshwater algae growth was suggested to be in the range of 6.8–10 [27, 28]. In this study, the inorganic N/P ratio of the effluent was 21, much higher than the optimal ratio, indicating the wastewater as phosphorus limitation media.

3.2. Growth of Scenedesmus sp. in Wastewater.

The green algae *Scenedesmus* sp. was cultivated in the wastewater for 10 days with different initial cell concentrations from 10 to 60 mg/L. The growth rate, Chl content, and flocculation

TABLE 1: The average composition of the wastewater (average ± SD of five samples).

Parameter	Unit	Value
pH		6.8 ± 0.5
Temperature	°C	29 ± 1.0
Dissolved oxygen (DO)	mg/L	4.7 ± 0.6
Ammonium (NH_4^+)	mg/L	26.5 ± 3.5
Nitrate (NO_3^-)	mg/L	11.3 ± 2.1
Phosphorus (PO_4^{3+})	mg/L	0.9 ± 0.28
Total nitrogen (TN)	mg/L	47.3 ± 5.9
Total phosphorus (TP)	mg/L	1.8 ± 0.27
Chemical oxygen demand (COD)	mg/L	180 ± 18
Biochemical oxygen demand (BOD_5)	mg/L	87 ± 12
Inorganic N/P		21

activity were presented in Table 2. The microalgae grew well in the wastewater with the growth rate from 0.30 to 0.38/day. There was no significant difference in the growth rate as the initial microalgae concentration increased from 10 to 60 mg/L. In the present study, wastewater was used as a nutrient medium for the growth of microalgae, and the utilization of nutrients allows wastewater treatment. During the growth phase, microalgae consumed mineral nutrients and CO_2 from wastewater to produce biomass and released O_2 into the medium [29].

Our results showed that flocculation activity increases with higher cell concentrations. Significant build up of flocculation activity (81.5 and 88.3%) was observed at the highest initial microalgae concentrations of 40 and 60 mg/L. Nguyen et al. [13] reported that the clear formation of flocculation occurred when *Chlorella vulgaris* in seafood wastewater with the initial concentration above 20 mg/L. Results of the present study are consistent with previous observations that higher initial biomass in the medium a better formation of flocculation because cell-cell encounters are more frequent, leading to better aggregation [30, 31]. Microalgal bioflocculation is an efficient low-cost technology for microalgal harvesting and wastewater treatment [14, 21, 32]. In general, the bioflocculation process is assisted with microorganisms (including bacteria, fungi, and yeasts) or their polymer substances [13–15]. Since no chemical is added in this process, the bioflocculation has been considered as a sustainable and green technique for algal biomass harvesting [14, 15]. The formation of algal flocculation and its application in wastewater treatment has been reviewed in detail [14, 15, 18]. In the present study, autoflocculation occurred when cultured *Scenedesmus* sp. in the wastewater for 10 days. Microalgal autoflocculation was found to be associated with increase in culture pH levels, due to CO_2 consumption by algal photosynthetic activity. Under these alkaline conditions, some metal ions precipitated together with the algal biomass [33]. Guo et al. [31] reported that cell wall-associated polysaccharides mediated self-flocculation of the microalga *S. obliquus*. Future study is needed in this area to understand the mechanism of self-flocculation of microalgal cells and increase application in wastewater treatment technology.

3.3. Removal of Nitrogen.

Nutrient removal in different initial biomass (from 10 to 60 mg/L), including (NH_4^+, NO_3^-, PO_4^{3-} and TP) during the experiment, are shown in Figure 2. The removal rate of NH_4^+ in the control (no microalgae) was 21.1%, and all treatment with *Scenedemsus* sp. achieved higher removal than in the control. The NH_4^+ and NO_3^- removal performance is shown in Figures 2(a) and 2(b) with the removal efficiencies from 71.7 to 92.8% and from 62.2 to 83.6%, respectively (Table 3). In general, the higher microalgal concentration resulted in higher removal efficiency of NH_4^+ and NO_3^-. This observation well agreed with previous studies that higher initial microalgae density enhanced nutrient uptake in different wastewater effluents [13, 34, 35]. Green algae can use a variety of nitrogen sources for growth, making it possible to use these algae for bioremediation to remove nitrogen from wastewater [26, 28]. Microalgae can convert different inorganic nitrogen forms from wastewater to organic nitrogen [15]. Previous studies have demonstrated that the major mechanisms of nitrogen removal in algae systems include nitrification or denitrification and biological uptake of nitrogen by dispersed biomass [34, 36].

Nitrification was observed during the first four days of the experiment; the decrease in ammonium concentration was accompanied by nitrate formation that peaked at day fourth and then decreased (Figures 2(a) and 2(b)). Although ammonium is the preferred nitrogen source for uptake, microalgae can consume nitrogen from a variety of nitrogen sources, including ammonium, nitrate, nitrite, and urea [26, 28, 36]. Since the removal efficiencies on nitrate are usually lower than those on ammonium, our results agree well with previous observations that green microalgae such as *Chlorella* and *Scenedemus* were the preference for ammonium to any other form of nitrogen present in wastewater [34, 37].

3.4. Removal of Phosphorus.

The removal rate of PO_4^{3-} and TP were shown in Table 3 and Figures 2(c) and 2(d). The percentages of PO_4^{3-} and TP removal for the control were only 17.5 and 26.8%, respectively. While in the treatment, this number ranged from 94.7% to 97.0% and from 75% to 95.8% for PO_4^{3-} and TP, respectively. The removal efficiencies were not significant differences ($P = 0.227$) as treating PO_4^{3-} with different concentrations of algal biomass. However, more significant TP removal rates were found during the treatment of wastewater with higher initial algae concentration (40 and 60 mg/L), compared with lower algae concentrations (10, 20, and 30 mg/L). The removal rates of TP were a significant correlation with the flocculation activities.

Removal of PO_4^{3-} up to 97% (Table 3) from wastewater treated with green algae *Scenedesmus* sp. was very effective. For all treatments, the concentration of PO_4^{3-} decreased gradually during ten days of the experiment (Figure 2(c)). But for TP, high removal rates were only found in the treatments with 40 or 60 mg/L. The concentration of TP did not decrease significantly during the first two days of the experiment but rapidly reduced from day 2 to day 6 of the test (Figure 2(d)).

TABLE 2: The growth rate, chlorophyll content, and flocculation activity.

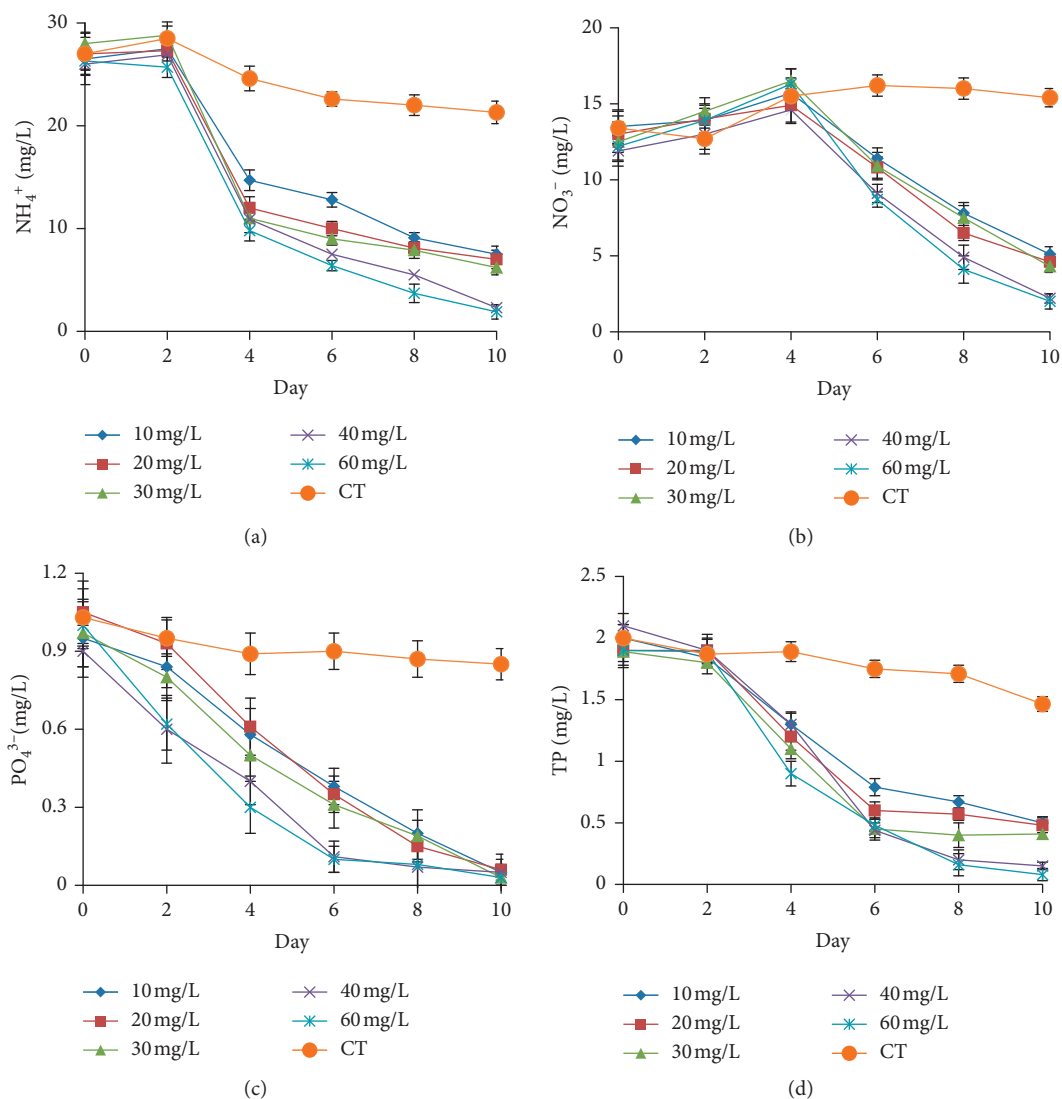|	Initial microalgae concentration (mg/L)				
	10 ± 0.9	20 ± 1.3	30 ± 1.6	40 ± 1.2	60 ± 1.5
Growth rate/day	0.3 ± 0.03	0.34 ± 0.02	0.36 ± 0.02	0.37 ± 0.03	0.38 ± 0.04
Chlorophyll (mg/L)	13.7 ± 1.8	14.5 ± 1.6	18.2 ± 1.9	19.4 ± 2.3	20.8 ± 2.5
Dry biomass (g/L)	30.5 ± 2.8	35.8 ± 3.3	42.1 ± 2.7	68.3 ± 3.6	70.2 ± 4.9
Flocculation activity (%)	14.2 ± 1.8	23.7 ± 4.3	41.6 ± 2.3	81.5 ± 5.7	88.3 ± 4.1

(a)

(b)
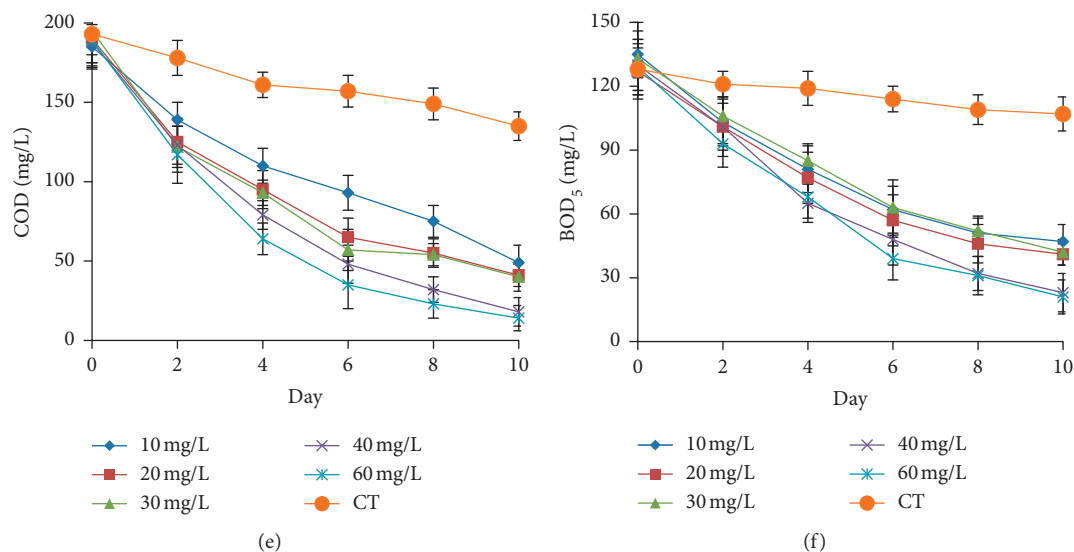

(c)

(d)

FIGURE 2: Continued.

(e)

(f)

FIGURE 2: Changes of NH_4^+ (a), NO_3^- (b), PO_{43}^- (c), TP (d), COD (e), and BOD5 (f) concentrations in the treatment with different initial microalgae concentrations.

TABLE 3: Flocculation activity and removal efficiency with different initial microalgae concentration.

Initial microalgae concentration	Flocculation activity (%)	Removal efficiency (%)					
		Ammonium	Nitrate	Phosphate	TP	COD	BOD_5
Control		21.1 ± 1.4	-14.9 ± 3.3	17.5 ± 2.1	26.8 ± 2.7	28.1 ± 2.0	16.4 ± 1.1
10 mg/L	14.2 ± 1.8	71.7 ± 1.9	62.2 ± 2.8	94.7 ± 1.5	75.0 ± 3.6	73.5 ± 3.4	65.2 ± 1.4
20 mg/L	23.7 ± 4.3	74.1 ± 2.1	64.6 ± 3.0	94.5 ± 2.3	74.7 ± 1.9	78.4 ± 2.4	67.7 ± 1.8
30 mg/L	51.6 ± 2.3	77.9 ± 2.7	65.6 ± 3.1	96.9 ± 2.8	78.3 ± 2.2	79.5 ± 4.4	68.4 ± 3.0
40 mg/L	81.5 ± 5.7	92.3 ± 4.3	81.5 ± 3.6	94.4 ± 2.2	92.9 ± 1.9	90.4 ± 4.1	82.3 ± 4.1
60 mg/L	88.3 ± 4.1	92.8 ± 3.5	83.6 ± 4.5	97.0 ± 1.7	95.8 ± 2.8	92.6 ± 4.0	83.7 ± 2.3

Table 3 shows the removal efficiency and flocculation activity at the end of the experiment. Compared with the control, the treatments with higher initial microalgae concentration had greater removal efficiencies and flocculation activities (Figure 3), showing a relationship between flocculation activity and removal efficiency. Previous studies have reported that the green algae *C. vulgaris* and *S. obliquus* could be used to remove PO_4^{3-} from the difference of wastewaters [15, 34, 35, 37]. Other studies suggested that the immobilized or flocculated form of microalgae is more effective than free form for nutrient removal in wastewater treatment [13, 15, 35, 38]. Our results are consistent with Nguyen et al. [13] that bioflocculation formation of microalgae enhanced nutrient removal from wastewater effluent. Naturally, phosphate seems to be depleted from the medium through different mechanisms including adsorption onto the cells surface, assimilation by the algae biomass or chemical precipitation [17, 34]. Previous studies have demonstrated that assimilation into biomass and adsorption were the main biotic processes of elimination of phosphorus in microalgae [17, 34].

3.5. *Removal of BOD_5 and COD.* The COD removal efficiencies varied a little among different initial microalgae concentrations (Figure 2(e)). While removal rates of only 73.5%, 78.4% and 79.5% were achieved for 10 mg/L, 20 mg/L and 30 mg/L of microalgae concentration, respectively, removal rates for 40 mg/L and 60 mg/L are up to 90.4% and 92.6%, respectively (Table 3). The concentration of COD decreased gradually during the experiment course. The removal rates of BOD_5 were almost the same trend with COD removal pattern and showed Figure 2(f). Higher removal rates were also found in the treatments with higher initial microalgae concentrations. There is a relationship between flocculation activity in the treatments with the removal efficiencies of COD and BOD_5. Higher flocculation activity resulted in higher removal rates in all treatments. Nguyen et al. [38] investigated the ability to removal of COD and BOD_5 in seafood wastewater; results indicated that the removal rates of COD and BOD_5 were 88% and 81%, respectively, under sunlight mode and 81% and 74% under fluorescent illumination, respectively, as clear formation of flocculation was observed. Previous studies reported that the presence of microalgae in the cultivation medium had increased the consumption of organic as well as inorganic matters [11, 38, 39]. Besides, Wang et al. [28] reported that two different metabolic pathways, i.e., heterotrophic and autotrophic growth of algae under different culture conditions. Green algae can perform heterotrophic growth besides the common autotrophic one of using CO_2 as the sole carbon source [40]. The organic substances may play as an
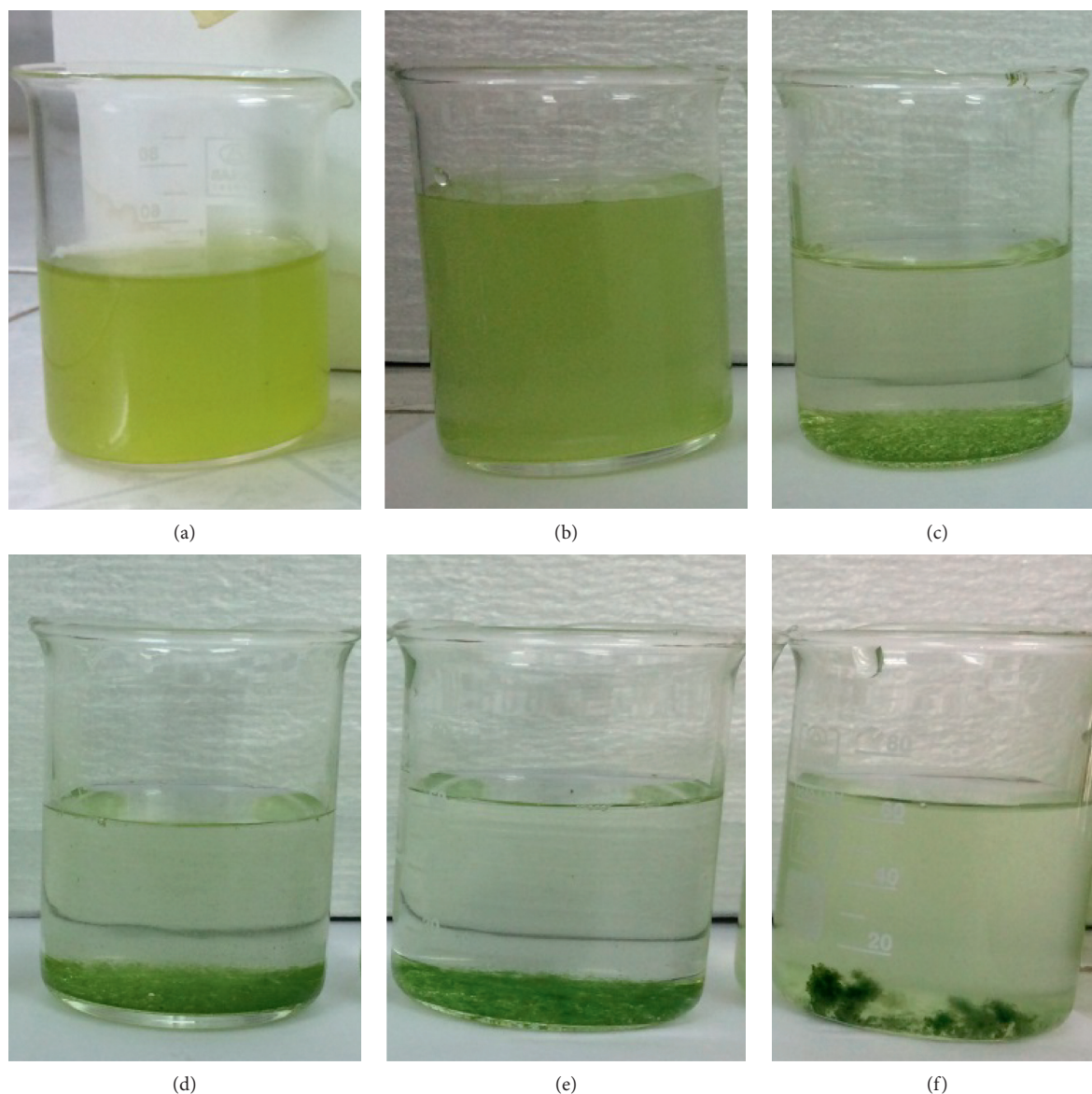
Figure 3: Flocculation activities in the control (a) and treatment with different concentrations of microalgae: 10 mg/L (b), 20 mg/L (c), 30 mg/L (d), 40 mg/L (e), and 60 mg/L (f).

essential organic nutrient for microalgae growth or act as an accessory growth factor. In green algae Chlorella, heterotrophic growth may occur in a much faster way by directly incorporating organic substrate in the oxidative assimilation process for storage material production [28], which is the reason why COD and BOD_5 concentration decreased after algal cultivation. Our results were also in line with the observations of Shen et al. [35] that green microalgae were able to utilize organic carbon for their metabolisms and assimilate organic compounds as a carbon source [41]. These results suggested that the wastewater could be used to provide sufficient nourishment to the algal cell for the metabolism process [42].

The microalgal-bacteria or fungi flocculation and its application in wastewater treatment have been investigated [13–15, 19, 20, 38], but little information is known about the autoflocculation of green algae in wastewater treatment. In this study, AFL occurred when the growth of the microalgae in the fertilizer plant wastewater. The flocculation was exceptionally high in the treatment with 40 and 60 mg/L of microalgae biomass. Nguyen et al. [38] observed that the AFL occurs when introducing the microgreen algae *C. vulgaris* in seafood wastewater after 8 days. AFL indicates the cell aggregation and adhesion of cells to each other in liquid culture. AFL can occur naturally in certain microalgae to response to some environmental stress such as changes in nutrients, pH, dissolved oxygen (DO), and amount of calcium and magnesium ions in the culture mediums [14]. It is reported that AFL was associated with increased pH due to the depletion of CO_2 concentration due to photosynthesis compared with precipitation of phosphate, magnesium, calcium, and carbonate salts with algal cells [13, 33].

In these treatments, the removal rates of nutrients, as well as COD and BOD_5, were relatively higher than other treatments, indicating that the AFL enhances the removal efficiencies. At the end of treatment, the two treatments with the most senior flocculation activities produced the most top elimination of nutrients, as well as COD and BOD_5. Similarly, higher removal percentages of nitrate, phosphates, and COD were reported to associate with bioflocculation process of microalgae [13, 18, 19, 38]. In general, algal cell density in flocculation forms is always higher than free forms [20, 21]. The high removal efficiency in wastewater treatment with AFL could be attributed to the availability of sufficient oxygen for further mineralization of organic carbon and nutrients because of the high concentration of microalga cells in flocculation formation. In addition, the growth and nutrient removal efficiency may depend on different mixed wavelength ratios. Zhao et al. [9] reported that *S. obliquus* and *C. Vulgaris* efficiently removed COD and TP from biogas slurry at a red : blue ratio of 5 : 5 but *S. obliquus* exhibited high N removal efficiency at a red : blue ratio of 7 : 3. Our results agree with reports by Tang et al. [17] who reported more nutrients, as well as COD and BOD_5 were removed in the treatments with the occurrence of flocculation of *C. vulgaris* compared with the treatment with only free cell form, indicating the enhancement of flocculation in pollutant removal. These results are also in accordance with the study conducted by Nguyen et al. [13] who reported that TSS removal efficiencies of treatment with no flocculation occurrence (20.6 ± 10.5%) were obviously lower than those with the clear formation of flocculation (90.0–95.0%).

4. Conclusion

The present results demonstrated the use of wastewater from a fertilizer plant in the cultivation and harvesting of *Scenedesmus* sp. Our results indicated that wastewater from fertilizer plants could be used as a cost-effective growth medium for algal biomass. The nutrient removal efficiency by *Scenedesmus* sp. isolated from the wastewater evidenced that microalgae are potential in removing nitrogen and phosphorous as well as COD and BOD_5 from a highly concentrated nutrient-rich such as fertilizer plant wastewater. The present study highlights the autoflocculation of microalgae could be used as a more practical alternative eco-friendly approach for wastewater treatment using microalgae to eliminate eutrophication.

Data Availability

The data used to support the findings of this study are included in the article.

Conflicts of Interest

The authors declare that there are no conflicts of interest regarding the publication of this paper.

Acknowledgments

References

[1] H.-P. Qin, Q. Su, S.-T. Khu, and N. Tang, "Water quality changes during rapid urbanization in the Shenzhen river catchment: an integrated view of socio-economic and infrastructure development," *Sustainability*, vol. 6, no. 10, pp. 7433–7451, 2014.

[2] A. L. Gonçalves, J. C. M. Pires, and M. Simões, "A review on the use of microalgal consortia for wastewater treatment," *Algal Research*, vol. 24, pp. 403–415, 2017.

[3] P. M. Glibert, "Eutrophication, harmful algae and biodiversity—challenging paradigms in a world of complex nutrient changes," *Marine Pollution Bulletin*, vol. 124, no. 2, pp. 591–606, 2017.

[4] J. M. O'Neil, T. W. Davis, M. A. Burford, and C. J. Gobler, "The rise of harmful cyanobacteria blooms: the potential roles of eutrophication and climate change," *Harmful Algae*, vol. 14, pp. 313–334, 2012.

[5] J. Heisler, P. M. Glibert, J. M. Burkholder et al., "Eutrophication and harmful algal blooms: a scientific consensus," *Harmful Algae*, vol. 8, no. 1, pp. 3–13, 2008.

[6] T.-L. Pham and M. Utsumi, "An overview of the accumulation of microcystins in aquatic ecosystems," *Journal of Environmental Management*, vol. 213, pp. 520–529, 2018.

[7] W. M. Lewis, W. A. Wurtsbaugh, and H. W. Paerl, "Rationale for control of anthropogenic nitrogen and phosphorus to reduce eutrophication of inland waters," *Environmental Science & Technology*, vol. 45, no. 24, pp. 10300–10305, 2011.

[8] N. C. Boelee, H. Temmink, M. Janssen, C. J. N. Buisman, and R. H. Wijffels, "Nitrogen and phosphorus removal from municipal wastewater effluent using microalgal biofilms," *Water Research*, vol. 45, no. 18, pp. 5925–5933, 2011.

[9] Y. Zhao, S. Sun, C. Hu, H. Zhang, J. Xu, and L. Ping, "Performance of three microalgal strains in biogas slurry purification and biogas upgrade in response to various mixed light-emitting diode light wavelengths," *Bioresource Technology*, vol. 187, pp. 338–345, 2015.

[10] L. E. González, R. O. Cañizares, and S. Baena, "Efficiency of ammonia and phosphorus removal from a colombian agro-industrial wastewater by the microalgae *Chlorella vulgaris* and *Scenedesmus dimorphus*," *Bioresource Technology*, vol. 60, no. 3, pp. 259–262, 1997.

[11] Y. Li, Y.-F. Chen, P. Chen et al., "Characterization of a microalga *Chlorella* sp. well adapted to highly concentrated municipal wastewater for nutrient removal and biodiesel production," *Bioresource Technology*, vol. 102, no. 8, pp. 5138–5144, 2011.

[12] S.-Y. Chiu, C.-Y. Kao, T.-Y. Chen, Y.-B. Chang, C.-M. Kuo, and C.-S. Lin, "Cultivation of microalgal *Chlorella* for biomass and lipid production using wastewater as nutrient resource," *Bioresource Technology*, vol. 184, pp. 179–189, 2015.

[13] T. D. P. Nguyen, T. V. A. Le, P. L. Show et al., "Bioflocculation formation of microalgae-bacteria in enhancing microalgae harvesting and nutrient removal from wastewater effluent," *Bioresource Technology*, vol. 272, pp. 34–39, 2019.

[14] S. B. Ummalyma, E. Gnansounou, R. K. Sukumaran, R. Sindhu, A. Pandey, and D. Sahoo, "Bioflocculation: an alternative strategy for harvesting of microalgae—an overview," *Bioresource Technology*, vol. 242, pp. 227–235, 2017.

[15] Y. Zhao, G. Guo, S. Sun, C. Hu, and J. Liu, "Co-pelletization of microalgae and fungi for efficient nutrient purification and biogas upgrading," *Bioresource Technology*, vol. 289, Article ID 121656, 2019.

[16] C. Alcántara, J. M. Domínguez, D. García et al., "Evaluation of wastewater treatment in a novel anoxic-aerobic algal-bacterial photobioreactor with biomass recycling through carbon and nitrogen mass balances," *Bioresource Technology*, vol. 191, pp. 173–186, 2015.

[17] C.-C. Tang, Y. Tian, H. Liang et al., "Enhanced nitrogen and phosphorus removal from domestic wastewater via algae-assisted sequencing batch biofilm reactor," *Bioresource Technology*, vol. 250, pp. 185–190, 2018.

[18] J. A. Gerde, L. Yao, J. Lio, Z. Wen, and T. Wang, "Microalgae flocculation: impact of flocculant type, algae species and cell concentration," *Algal Research*, vol. 3, pp. 30–35, 2014.

[19] M. Shahadat, T. T. Teng, M. Rafatullah, Z. A. Shaikh, T. R. Sreekrishnan, and S. Wazed Ali, "Bacterial bio-flocculants: a review of recent advances and perspectives," *Chemical Engineering Journal*, vol. 328, pp. 1139–1152, 2017.

[20] M. Agunbiade, C. Pohl, and O. Ashafa, "Bioflocculant production from *Streptomyces platensis* and its potential for river and waste water treatment," *Brazilian Journal of Microbiology*, vol. 49, no. 4, pp. 731–741, 2018.

[21] D. Vandamme, I. Foubert, and K. Muylaert, "Flocculation as a low-cost method for harvesting microalgae for bulk biomass production," *Trends in Biotechnology*, vol. 31, no. 4, pp. 233–239, 2013.

[22] V. M. Bhandari, L. G. Sorokhaibam, and V. V. Ranade, "Industrial wastewater treatment for fertilizer industry—a case study," *Desalination and Water Treatment*, vol. 57, no. 57, pp. 27934–27944, 2016.

[23] S. S. Kilham, D. A. Kreeger, S. G. Lynn, C. E. Goulden, and L. Herrera, "COMBO: a defined freshwater culture medium for algae and zooplankton," *Hydrobiologia*, vol. 377, no. 1/3, pp. 147–159, 1998.

[24] R. J. Ritchie, "Consistent sets of spectrophotometric chlorophyll equations for acetone, methanol and ethanol solvents," *Photosynthesis Research*, vol. 89, no. 1, pp. 27–41, 2006.

[25] L. S. Clesceri, A. E. Greenberg, A. D. Eaton et al., *Standard Methods for the Examination of Water and Wastewater*, American Public Health Association, Washington, DC, USA, 2012.

[26] O. Perez-Garcia, F. M. E. Escalante, L. E. de-Bashan, and Y. Bashan, "Heterotrophic cultures of microalgae: metabolism and potential products," *Water Research*, vol. 45, no. 1, pp. 11–36, 2011.

[27] C. S. Reynolds, *The Ecology of Freshwater Phytoplankton*, Cambridge University Press, Cambridge, UK.

[28] L. Wang, M. Min, Y. Li et al., "Cultivation of green algae *Chlorella* sp. in different wastewaters from municipal wastewater treatment plant," *Applied Biochemistry and Biotechnology*, vol. 162, no. 4, pp. 1174–1186, 2010.

[29] R. Muñoz and B. Guieysse, "Algal-bacterial processes for the treatment of hazardous contaminants: a review," *Water Research*, vol. 40, no. 15, pp. 2799–2815, 2006.

[30] E. M. Grima, E. H. Belarbi, F. G. Acién Fernández, A. Robles Medina, and Y. Chisti, "Recovery of microalgal biomass and metabolites: process options and economics," *Biotechnology Advances*, vol. 20, no. 7-8, pp. 491–515, 2003.

[31] S.-L. Guo, X.-Q. Zhao, C. Wan et al., "Characterization of flocculating agent from the self-flocculating microalga *Scenedesmus obliquus* AS-6-1 for efficient biomass harvest," *Bioresource Technology*, vol. 145, pp. 285–289, 2013.

[32] C. Wan, M. A. Alam, X.-Q. Zhao et al., "Current progress and future prospect of microalgal biomass harvest using various flocculation technologies," *Bioresource Technology*, vol. 184, pp. 251–257, 2015.

[33] A. Sukenik and G. Shelef, "Algal auto-flocculation—verification and proposed mechanism," *Biotechnology and Bioengineering*, vol. 26, no. 2, pp. 142–147, 1984.

[34] L. Delgadillo-Mirquez, F. Lopes, B. Taidi, and D. Pareau, "Nitrogen and phosphate removal from wastewater with a mixed microalgae and bacteria culture," *Biotechnology Reports*, vol. 11, pp. 18–26, 2016.

[35] Y. Shen, J. Gao, and L. Li, "Municipal wastewater treatment via co-immobilized microalgal-bacterial symbiosis: microorganism growth and nutrients removal," *Bioresource Technology*, vol. 243, pp. 905–913, 2017.

[36] Q. Dortch, "The interaction between ammonium and nitrate uptake in phytoplankton," *Marine Ecology Progress Series*, vol. 61, pp. 183–201, 1990.

[37] A. Ruiz-Marin, L. G. Mendoza-Espinosa, and T. Stephenson, "Growth and nutrient removal in free and immobilized green algae in batch and semi-continuous cultures treating real wastewater," *Bioresource Technology*, vol. 101, no. 1, pp. 58–64, 2010.

[38] T. D. P. Nguyen, T. N. T. Tran, T. V. A. Le, T. X. Nguyen Phan, P.-L. Show, and S. R. Chia, "Auto-flocculation through cultivation of *Chlorella vulgaris* in seafood wastewater discharge: influence of culture conditions on microalgae growth and nutrient removal," *Journal of Bioscience and Bioengineering*, vol. 127, no. 4, pp. 492–498, 2019.

[39] I. Woertz, A. Feffer, T. Lundquist, and Y. Nelson, "Algae grown on dairy and municipal wastewater for simultaneous nutrient removal and lipid production for biofuel feedstock," *Journal of Environmental Engineering*, vol. 135, no. 11, pp. 1115–1122, 2009.

[40] E. R. Burrell, E. W. Inniss, and I. C. Mayfield, "Development of an optimal heterotrophic growth medium for Chlorella vulgaris," *Applied Microbiology and Biotechnology*, vol. 20, no. 4, pp. 281–283, 1984.

[41] G. Mujtaba and K. Lee, "Advanced treatment of wastewater using symbiotic co-culture of microalgae and bacteria," *Applied Chemical Engineering*, vol. 27, no. 1–9, 2016.

[42] X. Ma, W. Zhou, Z. Fu et al., "Effect of wastewater-borne bacteria on algal growth and nutrients removal in wastewater-based algae cultivation system," *Bioresource Technology*, vol. 167, pp. 8–13, 2014.